Growth and photorefractive properties of an Fe-doped near-stoichiometric $LiNbO_3$ crystal

2005 J. Phys. D: Appl. Phys. 38 2013

(http://iopscience.iop.org/0022-3727/38/12/024)

INSTITUTE OF PHYSICS PUBLISHING JOURNAL OF PHYSICS D: APPLIED PHYSICS

J. Phys. D: Appl. Phys. **38** (2005) 2013–2016 doi:10.1088/0022-3727/38/12/024

Growth and photorefractive properties of an Fe-doped near-stoichiometric $LiNbO_3$ crystal

Tao Zhang, Biao Wang[1], Shuangquan Fang and Decai Ma

Electro-Optics Technology Center, Harbin Institute of Technology, Harbin 150001, People's Republic of China

E-mail: tzhang_hit02@yahoo.com

Received 5 August 2004, in final form 25 February 2005
Published 3 June 2005
Online at stacks.iop.org/JPhysD/38/2013

Abstract

A near-stoichiometric $LiNbO_3$ crystal with 0.02 wt% Fe_2O_3 doping was grown from a Li-rich melt (Li/Nb = 1.38, atomic ratio) by the Czochralski method in air atmosphere. The OH^- absorption band was characterized by infrared transmittance spectra. The appearance of the 3466 cm^{-1} absorption band (2.89 μm) manifests that the composition of the grown crystal is close to the stoichiometric ratio. The photorefractive properties were measured by a two-wave coupling experiment. The measured results show that the Fe-doped near-stoichiometric $LiNbO_3$ crystal has a larger exponential gain coefficient than the Fe-doped congruent $LiNbO_3$ crystal. The remarkable gain can be attributed to the photovoltaic field being comparable with the effective limiting space-charge field.

1. Introduction

Lithium niobate ($LiNbO_3$, LN) possesses excellent electro-optics, ferroelectric, piezoelectric, acoustic and nonlinear properties, and is a promising material for many applications in second harmonic generation (SHG) [1], holographic data storage [2], optical parametric oscillation [3] and coherent optical amplification [4]. Congruent $LiNbO_3$ crystals generally have good optical quality and uniformity; however, being a typical non-stoichiometric composition, a high concentration of intrinsic defects, i.e. anti-site Nb_{Li} (Nb occupied Li site) and V_{Li} (Li vacancy) according to the Li-site vacancy model [5, 6], are always present in crystals. Usually, the pure congruent $LiNbO_3$ has little practical applications in the above-mentioned aspects because of its many serious disadvantages such as low threshold for optical damage, low diffraction efficiency, low sensitivity and long response time.

So far, three main methods have been developed to improve the photorefractive performance in $LiNbO_3$. One is by doping various impurity ions to tailor the properties of $LiNbO_3$ crystals, such as Fe [7], Ce [8], Mn [9], Cu [10], Mg [11], Zn [12], In [13], Sc [14] and so on. Another is by means of post-growth treatments (reduction or oxidation) to improve the photorefractive properties [15, 16]. In addition, the control of the Li/Nb ratio in $LiNbO_3$ crystals has been demonstrated to be of key importance for the improvement of their properties [17, 18]. The near-stoichiometric $LiNbO_3$ (SLN) crystal is expected to have fewer defects and superior behaviours because of its more ideal structure in the crystal ([Li]/[Nb] $\approx$ 1, atomic ratio); therefore the near-stoichiometric $LiNbO_3$ crystal has been widely studied in the past few years. In two-wave coupling experiments, undoped or doped near-stoichiometric $LiNbO_3$ crystals have a larger exponential gain coefficient, faster response speed and higher sensitivity than doped congruent ones. However, the corresponding mechanisms are still unclear.

In this paper, we choose transition element Fe for increasing the photorefractive effect to grow an Fe-doped near-stoichiometric $LiNbO_3$ single crystal from a Li-rich melt by the Czochralski method. The infrared (IR) transmittance spectra and photorefractive properties in Fe : SLN were measured and compared with Fe : CLN, and the underlying mechanisms were discussed.

[1] Author to whom any correspondence should be addressed.

2. Experimental methods

2.1. Crystal growth and sample preparation

The raw materials for crystal growth are $LiCO_3$, Nb_2O_5, Fe_2O_3 with the purity of 4N. The Li-rich materials of Li/Nb = 1.38 (atomic ratio) and 0.02 wt% Fe_2O_3 doping were selected as the starting melt compositions to grow an Fe-doped near-stoichiometric $LiNbO_3$ crystal (Fe : SLN) by the convenient Czochralski method in air atmosphere. In order to form a polycrystalline bulk, the raw materials were precisely weighed, thoroughly mixed for 12 h, and fully calcined at 700°C for 2 h and then sintered at 1150°C for 2 h, respectively. The initial weight of the reacted materials that were charged in a platinum crucible, 80 mm in diameter and 50 mm in height, was approximately 1000 g. To obtain a high homogeneity crystal, the crystal growth was abruptly stopped when about 5 wt% of the initial charge had been pulled out. The transparent, crack-free and inclusion-free crystal, ∼25 mm in diameter and ∼25 mm in length, was grown under the optimum growth parameters: pulling rate of 0.3 mm h^{-1}, seed rotation rate of ∼15 rpm and temperature gradient of ∼20°C cm^{-1}. After growth, the crystal was cooled to room temperature at a rate of 80°C h^{-1}. In order to compare with the actual investigation, a congruent $LiNbO_3$ (Fe : CLN) crystal of the same doping level was also grown.

It was found by an etching experiment [19] that as-grown Fe : SLN had almost single ferroelectric domain structures. For optical characterization, the two crystals were y-cut into slices of dimensions $10 \times 2 \times 10\,mm^3$ ($a \times b \times c$) from the middle, then polished to optical grade smoothness. Lastly, the samples were short circuited to avoid space charge accumulation in all experiments by covering the other four faces (x, z) with silver paste.

2.2. Measurements

The IR transmittance spectra of the crystals were recorded with a Fourier spectrophotometer at room temperature. The measurement wavenumber range was from 3000 to 4000 cm^{-1}.

Holographic measurements were performed with a two-wave coupling experiment at room temperature. A schematic diagram of the experimental set-up is shown in figure 1. Two mutually coherent and extraordinarily polarized green beams from a doubled Nd : YAG laser ($\lambda = 532$ nm) were used as writing beams, i.e. signal beam S and reference beam R. The grating vector of written holograms was set along the crystal's c-axis to utilize the largest electro-optic coefficient γ_{33}. The intensity ratio of S to R could be adjusted by rotation of the half-wave plate HW_1. The diffraction efficiency η was monitored during the recording process with a weak beam of a He–Ne laser ($\lambda = 633$ nm, ordinary polarization) that was Bragg matched.

3. Experimental results and discussion

3.1. IR spectra analysis

It was reported that the location of the OH^- absorption peak usually has a strong relationship with Li concentration in the crystal [20, 21]. Figure 2 shows the IR transmittance spectra of Fe : SLN and Fe : CLN crystals. The congruent crystal presents a broad non-symmetrical absorption band (FWHM about 30 cm^{-1}) at approximately 3482 cm^{-1}. But in Fe : SLN the absorption band is shifted to a narrow line at 3466 cm^{-1} (FWHM less than 5 cm^{-1}). The appearance of the 3466 cm^{-1} absorption band (2.89 μm) manifests that the grown crystal is close to the stoichiometry, since this band occurs only in near-stoichiometric $LiNbO_3$.

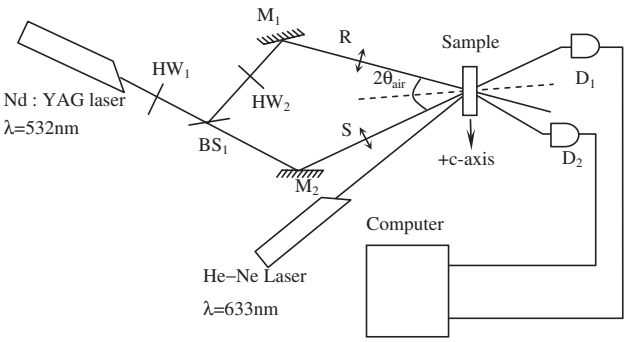

Figure 1. Scheme of two-wave coupling experimental set-up. M_1, M_2: mirrors; BS_1: beam splitter; D_1, D_2: detectors; R: reference beam; S: signal beam; HW_1, HW_2: half-wave plates.

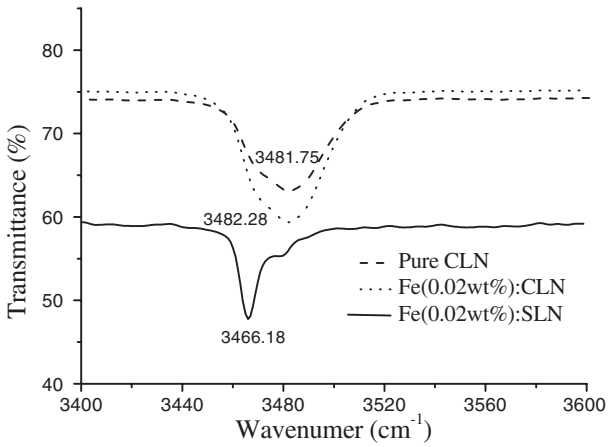

Figure 2. The IR transmittance spectra of the crystals.

3.2. Diffraction efficiency

The holographic gratings were recorded with two beams (S, R) of equal intensity up to 450 mW cm^{-2} at an intersection angle of ∼15.3° on the incident crystal surface (see figure 1). The diffraction efficiency η is defined as the diffracted intensity I_d of the probe laser beam divided by the corresponding transmitted intensity I_t, i.e. $\eta = I_d/I_t \times 100\%$. The corresponding refractive index change Δn and the space-charge field E_{sc} are calculated by Kogelnik's formula [22] and electro-optic effect, respectively. At the same time, the amplitude of the diffuse field E_d can be determined as

$$E_d = \frac{2\pi k_B T}{e\Lambda}, \tag{1}$$

where k_B is Boltzmann's constant, e is the electron charge, T the absolute temperature and Λ the grating period. The experimental results are shown in table 1.

Table 1. Summary of the photorefractive properties for crystals.

Sample	Diffraction efficiency, $\eta(\%)$	Refractive index, Δn	Space-charge field, E_{sc} ($V\,cm^{-1}$)	Diffusion field, E_d ($V\,cm^{-1}$)
Fe : CLN	78	9.15×10^{-5}	5.36×10^3	792
Fe : SLN	55	7.06×10^{-5}	4.11×10^3	792

As is well-known, the photorefractive process in $LiNbO_3$ has been attributed to a photovoltaic effect, to diffusion and to drift of photo-carriers. The photovoltaic effect, presumably based on the polarity of the lattice, accounts for photocurrents along the polar axis even in the absence of applied fields. The diffusion current results from the density gradient of free charge carriers by inhomogeneous illumination, whereas the drift current is due to the Coulomb interaction of an electric field with the photo-carrier. It can be seen from table 1 that the space-charge field E_{sc} is larger than the diffusion field E_d; therefore, the additional contribution to E_{sc} is obviously the photovoltaic field, i.e. the photovoltaic field is the dominant effect during the recording process for the two crystals.

3.3. Exponential gain coefficient

The two-wave coupling experiment was employed to obtain the steady-state exponential gain coefficient Γ (see figure 1). The total beam intensity was $900\,mW\,cm^{-2}$. The reference–signal intensity ratio m was adjusted to 250 by rotation of the half-wave plate HW_1. By measuring the signal beam intensity I_s (I_s') after the beam passes through the crystal, with (without) coupling to the reference beam, the amplification γ is obtained from the relation

$$\gamma = \frac{I_s}{I_s'}. \tag{2}$$

The exponential gain coefficient Γ is experimentally measured through the equation [23]

$$\Gamma = \frac{1}{L} \ln\left[\frac{m\gamma}{1+m-\gamma}\right], \tag{3}$$

where L is the interaction length of two incident beams in the crystal and m is the reference–signal intensity ratio. Figure 3 shows the dependence of the exponential gain coefficient Γ on the grating period Λ. It is found in Fe : SLN that the gain increases quickly with the increase in grating period in the range of small periods, and reaches the maximum value $27\,cm^{-1}$ at $\Lambda = 1.8\,\mu m$, and then decreases with increase in Λ. In contrast, in Fe : CLN, the gain change with grating period is not as obvious as in Fe : SLN, and its maximum gain ($\Gamma_{max} = 15\,cm^{-1}$) is reduced by a fraction of ~ 2 compared with that of Fe : SLN.

In fact, the photovoltaic field E_{ph} in the measurement range of the grating periods exceeds the diffuse field E_d. Thus, the diffuse field E_d can be negligible in the photorefractive effect for the two crystals. According to the theory of two-wave coupling, the exponential gain coefficient Γ defined in equation (3) is given by [24]

$$\Gamma = \frac{2\pi n^3 \gamma_{eff} \cos(2\theta)\cos(\theta)}{\lambda} \frac{E_s' E_{ph}^2}{E_s'^2 + E_{ph}^2} \tag{4}$$

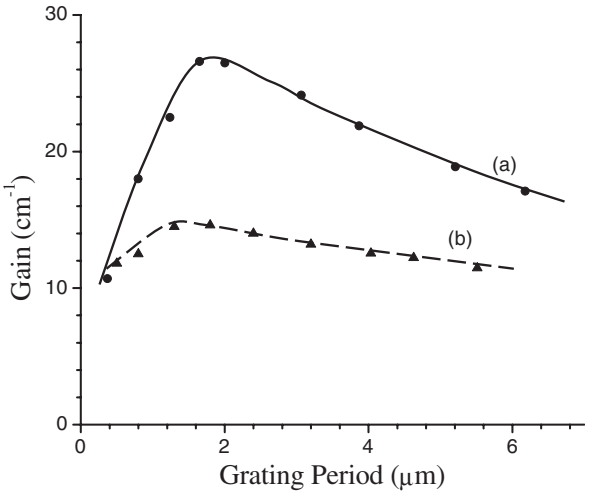

Figure 3. Experimental curves of Γ versus Λ. (a) Fe_2O_3 (0.02 wt%) : SLN; (b) Fe_2O_3 (0.02 wt%) : CLN. The lines represent the fitting curves by the formula (4).

Table 2. Fitting data for the two crystals.

Sample	Maximum gain, Γ_{max} (cm^{-1})	Grating period, $\Lambda(\mu m)$	Photovoltaic field, E_{ph} ($V\,cm^{-1}$)	Filled trap density, N^- (cm^{-3})
Fe : CLN	15	1.8	5.83×10^3	3.0×10^{16}
Fe : SLN	27	1.6	4.21×10^3	2.6×10^{15}

with

$$E_s' = E_s \frac{N}{N^0}, \tag{5}$$

and

$$E_s = \frac{e\Lambda}{2\pi\varepsilon\varepsilon_0} \frac{N^0}{N} N^-, \tag{6}$$

where E_s, E_s' and E_{ph} are the limiting space-charge field, effective limiting space-charge field and photovoltaic field, respectively; N^-, N^0, N are the filled trap density, empty trap density and total trap density, respectively; n is the refractive index; θ is half of the angle between the recording beams inside the crystal; γ_{eff} is the effective electro-optic coefficient; λ is the recording wavelength in vacuum; and $\varepsilon\varepsilon_0$ is the dielectric constant of the $LiNbO_3$ crystal. The phase shift φ between the holographic grating and interference pattern is given by

$$\tan\varphi = \frac{E_{ph}}{E_s'} \propto \frac{E_{ph}}{\Lambda N^-}. \tag{7}$$

It is very clear that the exponential gain coefficient Γ in equation (4) is a function of the photovoltaic field E_{ph}, filled trap density and grating period Λ. Fitting this expression to the experimental data of gain Γ by the least-square method, the parameters E_{ph} and N^- can be obtained. Figure 3 shows the fitting curve and, as we can see, the fit is very good. Table 2 lists the fitting values of E_{ph} and N^- for the two crystals.

From figure 3, the following conclusions can be easily obtained in the Fe : SLN crystal: (1) when the grating period Λ is a little small, the photovoltaic field E_{ph} is much larger than the effective limiting space-charge field E_s', so the gain Γ is proportional to E_s' and therefore to Λ by equation (4); i.e. Γ increases linearly with the increase of Λ; (2) when

Λ is a little large, E_{ph} is much smaller than E_s', so Γ is inversely proportional to E_s' and therefore to Λ by equation (4), i.e. decreases with increase in Λ; and (3) when Λ is exactly equal to 1.8 μm, E_{ph} is equal to E_s' and Γ reaches its maximum.

It is well known that a phase shift between the holographic grating and the interference pattern is necessary to get a steady-state energy transfer from the reference beam to the signal beam. The fitting results (as shown in table 2) indicate that there is a large photovoltaic field and a small filled trap density in Fe : SLN, which results in the photovoltaic field being comparable with the effective limiting space-charge field in our measurement range, so a large steady-state energy transfer ($\Gamma_{max} = 27\,cm^{-1}$) takes place due to equation (7). In contrast, though the photorefractive effect in Fe : CLN is also governed by the photovoltaic field, the filled trap density is so large that the photovoltaic field is much smaller than the effective limiting space-charge field in the measurement; thus the phase shift is close to zero by equation (7), and there only exists a small steady-state energy transfer ($\Gamma_{max} = 15\,cm^{-1}$) in Fe : CLN.

4. Conclusion

Fe-doped near-stoichiometric $LiNbO_3$ crystals grown from a Li-rich melt by the Czochralski method were studied and compared with Fe : CLN. The IR spectra demonstrate that this grown crystal is near the stoichiometry, and shows that its absorption band becomes narrow and shifts towards lower wave numbers (3466 cm^{-1}). The exponential gain coefficient of Fe : SLN is much larger than that of Fe : CLN. The main reason is that the photovoltaic field is comparable with the effective limiting space-charge field in Fe : SLN.

Acknowledgments

This work is financially supported by the Chinese Advanced Technology Program No 863 (2001AA31304), Chinese Research for Fundamental Key Projects No 973 (G19990330), Chinese Natural Science Foundation (10172030, 50232030) and the Nature Science Foundation of Heilongjiang Province (A01-01).

References

[1] Li M H, Xu Y H, Wang R, Zhen X H and Zhao C Z 2002 *Cryst. Res. Technol.* **36** 191
[2] Chen C T, Kim D M and von der Linde D 1979 *Appl. Phys. Lett.* **34** 321
[3] Myers L E, Miller G D, Eckardt R C, Fejer M M, Byer R L and Bosenber W R 1995 *Opt. Lett.* **20** 52
[4] Capmany J, Jaque D, Sanz García J A and García Solé J 1999 *Opt. Commun.* **161** 253
[5] Iyi N, Kitamura K, Yajima Y and Kimura S 1995 *J. Solid State Chem.* **118** 148
[6] Iyi N, Kitamura K, Izumi F, Yamamoto J K, Hayashi T, Asano H and Kimura S 1992 *J. Solid State Chem.* **101** 340
[7] Burr G W and Psaltis D 1996 *Opt. Lett.* **21** 893
[8] Yang C H, Zhao Y Q, Wang R and Li M H 2000 *Opt. Commun.* **175** 247
[9] Yang Y P, Psaltis D, Luennemann M, Berben D, Hartwig U and Buse K 2003 *J. Opt. Soc. Am.* B **20** 1491
[10] Imbrock J, Wirp A, Kip D and Krätzig E 2002 *J. Opt. Soc. Am.* B **19** 1822
[11] Sweeney K L, Hallibuton L E and Bryan D A 1985 *J. Appl. Phys.* **57** 1036
[12] Volk T, Pryalkin V I and Rubinina N M 1990 *Opt. Lett.* **15** 996
[13] Volk T, Rubinina N and Wohlecke M 1994 *J. Opt. Soc. Am.* B **11** 1681
[14] Yamanoto J K, Kitamura K, Iyi N, Kimura S, Furukawa Y and Sato M 1992 *Appl. Phys. Lett.* **61** 2156
[15] Chen X J, Zhu D S, Li B, Ling T and Wu Z K 2001 *Opt. Lett.* **26** 998
[16] Hatano H, Yamaji T, Tanaka S, Furukawa Y and Kitamura K 1999 *Japan. J. Appl. Phys.* **38** 1820
[17] Xu Y H, Xu W S, Xu S W and Wang B 2003 *Opt. Mater.* **23** 305
[18] Zhen X H, Xu W S, Zhao C Z, Zhao L C and Xu Y H 2002 *Cryst. Res. Technol.* **37** 976
[19] Furukawa Y, Kitamura K, Takekawa S, Niwa K, Yajima Y, Iyi N, Mnushkina I, Guggenheim P and Martin J M 2000 *J. Cryst. Growth* **211** 230
[20] Polgar K, Peter A, Kovacs L, Corradi G and Szaller Zs 1997 *J. Cryst. Growth* **177** 211
[21] Guenther H, Macfarlane R, Furukawa Y, Kitamura K and Neurgaonkar R 1998 *Appl. Opt.* **37** 7611
[22] Kogelnik H 1969 *Bell Syst. Tech. J.* **48** 2909
[23] Furukawa Y, Kitamura K and Ji Y 1997 *Opt. Lett.* **22** 501
[24] Kukhatare N V, Markov V B, Odulov S G, Soskin M S and Vinetskii V L 1979 *Ferroelectrics* **22** 949